

We are IntechOpen, the world's leading publisher of Open Access books Built by scientists, for scientists

4,800

Open access books available

122,000

International authors and editors

135M

Downloads

Our authors are among the

154

Countries delivered to

TOP 1%

most cited scientists

12.2%

Contributors from top 500 universities



WEB OF SCIENCE™

Selection of our books indexed in the Book Citation Index
in Web of Science™ Core Collection (BKCI)

Interested in publishing with us?
Contact book.department@intechopen.com

Numbers displayed above are based on latest data collected.
For more information visit www.intechopen.com



Inorganic–Organic Perovskite Solar Cells

Sohrab Ahmadi Kandjani, Soghra Mirershadi and
Arash Nikniaz

Additional information is available at the end of the chapter

<http://dx.doi.org/10.5772/58970>

1. Introduction

The most of modern commercial optoelectronic devices such as Laser diodes, solar cells, light-emitting diodes (LEDs), and nonlinear optical devices are built on the basis of traditional inorganic semiconductors. However, a lot of progress has been made in producing devices based on organic electronic materials, in recent decades [1], but the current development prospects of organic materials are mostly limited in their scope to relatively low-performance areas. Low mobility of charge carriers in molecular materials, can be mentioned as one of import reason for this topic. Strong chemical interaction between organic molecules and metal electrodes can destroy the injection of charge carriers into the organic molecules [2].

A qualitatively different way of using organic electronic compounds can be *via* exploiting resonant interactions in organic-inorganic hybrid structures [3–5]. Within the same hybrid structure, one could combine high conductivity of the inorganic semiconductor component with the strong light-matter interaction of the organic component. However, this properties classified them as named organic-inorganic hybrid materials with large exciton binding energy (about several hundreds of meV) because of large dielectric confinement. These layered organic-inorganic perovskites with the general formula $(\text{RNH}_3)_2\text{MX}_4$ ($\text{R} = \text{C}_n\text{H}_{2n+1}$; $\text{M} = \text{Pb}$ or Sn ; $\text{X} = \text{halogen}$), can be regarded as semiconductor/insulator multiple quantum well systems consisting of lead halide semiconductor layers sandwiched between organic ammonium insulator layers [6–10]. Lead halide is well known as typical ionic crystals with a large exciton binding energy (a few tens of meV) [11]. Further, the organic layer has a larger band gap and lower dielectric constant than those of the inorganic layer. Therefore, the exciton binding energy is considerably amplified due to the quantum and dielectric confinement effects [12]. As a result, stable excitons are observed even at room temperature. Thus, the appropriate properties of both the organic and the inorganic materials can exploited to overcome their

limitations when used separately. The lead halide based organic-inorganic perovskites have potential applications in nonlinear optical devices [13,14] and novel luminescent devices [15,16]. Organometallic halide perovskites have recently emerged as a promising material for high-efficiency nanostructured devices [17]. Over the past several months, we have witnessed an unanticipated breakthrough and rapid progress in the field of developing photovoltaics, with the realization of highly efficient solar cells based on organometallic trihalide perovskite absorbers [18–21].

Simplified schematic representation of the crystal structure of the organic-inorganic hybrids as shown in Figure 1. The two-dimensional inorganic layers and an organic ammonium layer are stacked alternately. These layers is comprised of a two-dimensional sheet of $[MX_6]^{-4}$ octahedra which are connected at the four corners with halide ions on the plane.

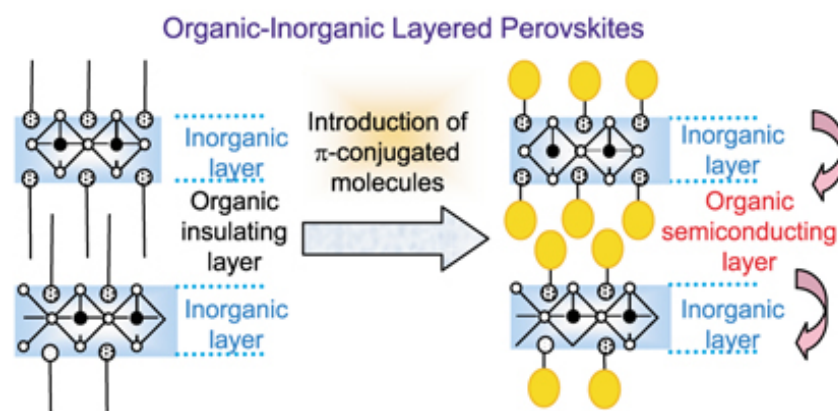


Figure 1. Schematic structure of the organic-inorganic hybrid crystal

As shown in Figure 2, the six halogen ions X^- surrounded M^{2+} , forming an octahedral $[MX_6]^{-4}$ cluster. The inorganic layer has thickness of a few atomic layers. The $-\text{NH}_3^+$ ends of the cations bind to the anion layers of $[MX_6]^{-4}$ in a specific orientation determined by hydrogen bonding with both equatorial and axial halide ions. A multi-layer structure is organized by neutralizing $[MX_6]^{-4}$ with alkylammonium ions [24].

Also Perovskites Material use as solar cell in last few years as show in Figure 3. The reasons for make them as one of best candidate for photovoltaics is explain below:

1. Appropriate Material properties of high efficiency photovoltaics
2. High coefficient of optical absorption
3. Excellent charge carrier transportation
4. Promising device parameters
5. Stability for maintain more than 80% of its initial efficiency after 500 hours.
6. Lower manufacturing costs because of directly deposition from solution

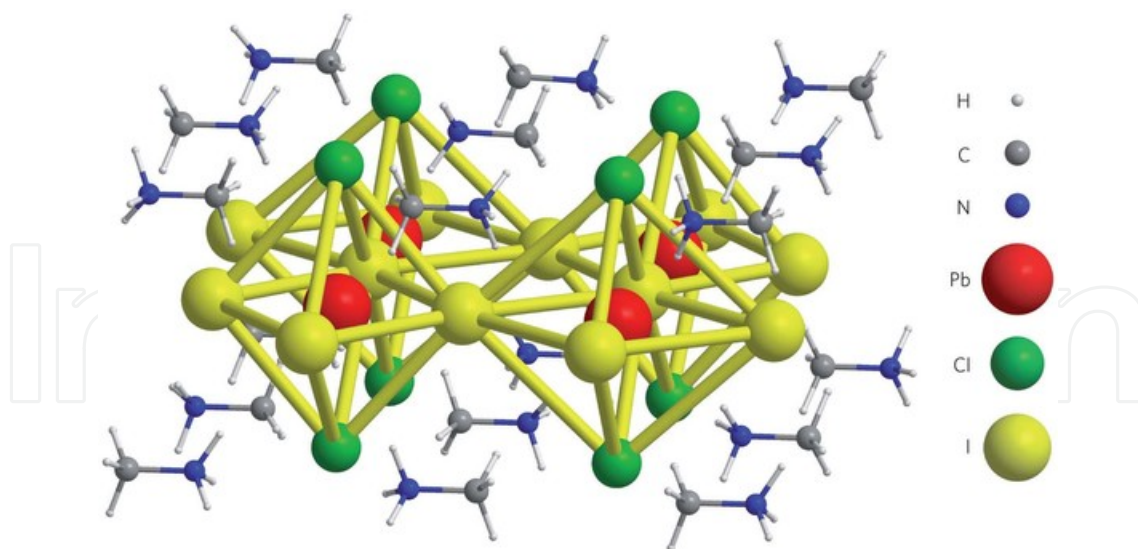


Figure 2. Schematic of the cluster structure of the organic-inorganic hybrid []

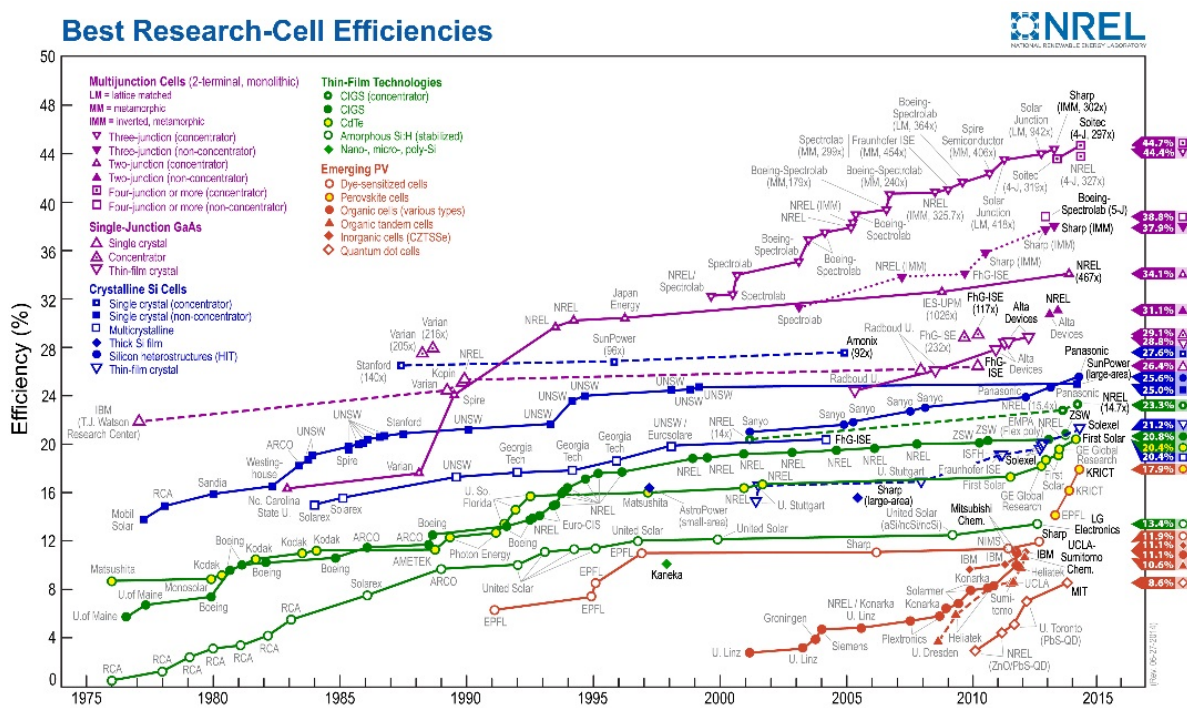


Figure 3. Best research cell efficiencies of all type of solar cells (NREL)

2. Synthesis of inorganic–organic solar cells materials

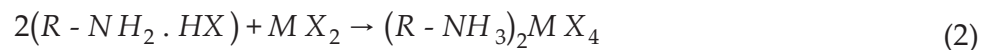
The synthesis of perovskites is the main and important procedure among perovskites study. Compared with the common semiconductors, the fabrication of perovskites samples is relatively easy. Because the crystals of perovskites molecules can form spontaneously via self-

assembly process and they need neither intricate equipment nor confined environment condition but can be synthesized and deposited simply by soft chemical methods at room temperature. Generally there are two steps for synthesis: synthesis of ammonium salts and preparation of perovskites solution.

In the first step, for the perovskites that are mainly in form of $(R-NH_3)_2MX_4$, the as-prepared amines transform to ammonium salts by reacting the amines with halogen acid. This neutralization reaction where the salts are generated is described in formula 1:



The halogen acids used to produce corresponding ammonium salts are HI 57 wt%, HBr 48 wt% or HCl 37 wt% aqueous solution. After several days of drying in desiccator, the salts are dry. These dry ammonium salts are used to prepare perovskites solution. In this step, $R - NH_2 \cdot HX$ ammonium salt is mixed with lead halide PbX_2 in stoichiometric amount in mole, and dissolved in solvent. This is a coordination reaction and it can be described by the chemical formula: 2:



The solution is then put under agitation or in ultrasonic bath until the solutes are totally dissolved and the solution appears limpid. From the perovskites solution, 2D crystals can be obtained by evaporation of solvent by self-organization process. The solvent containing $R - NH_2 \cdot HX$ and MX_2 is first spin-coated on the substrate. 2D layered perovskites crystals are then obtained upon solvent evaporation. In the absorption spectra of 2D layered perovskites crystals, a sharp peak appears at room temperature, which is characteristic of the formation of 2D layered perovskites crystal structure [25].

Another method to synthesis of perovskites is two-step based on the layer-by-layer technique. For example, thin films of microcrystalline $(C_8H_{17}NH_3)_2PbBr_4$ are prepared by the two-step growth process by Kitazawa et.al as follows: (1) precipitation of nanometer-sized $PbBr_2$ particles on substrates by vapor deposition and then (2) growth of $(C_8H_{17}NH_3)_2PbBr_4$ films by exposing $PbBr_2$ particles to $C_8H_{17}NH_3Br$ vapor. A simple vacuum chamber is used as a deposition apparatus with about 8×10^{-6} Torr as Background pressure. This chamber is attached to a vacuum system, two-independent thermal evaporation sources, a shutter and a substrate holder. The thermal evaporation source consists of a quartz cell coiled with a tantalum wire. First of all, $PbBr_2$ particles are deposited on Si (100) substrates by vapor deposition. Next, $PbBr_2$ particles are exposed to $C_8H_{17}NH_3Br$ vapor for growing of $(C_8H_{17}NH_3)_2PbBr_4$ films. Exposure time is varied from 0 to 600 s. The substrate temperature is kept at room temperature during deposition. Thin films of microcrystalline that prepared by the two-step growth process and their optical properties are dependent on the exposure time [12].

Perovskites in form of luminescent nanoparticles are another remarkable kind of crystals which has attracted excessive attention recently. Between bulk materials and atomic or molecular structures, the nanoparticles show very specific properties with potential applica-

tions in various fields such as sensing or LEDs. Nanoparticles often have specific optical properties as they are small enough to confine their electrons and produce quantum effects. Thus, the fabrication method which chooses the size of nanoparticles is very vital. For the first time Audebert et al. have realized luminescent nanoparticles by a spray-drying method. In brief, the ammonium salts and PbBr_2 or PbI_2 semiconductors are firstly dissolved in DMF solvent and used for the nanoparticles spray drying. The experimental spray drier is composed of an aerosol generator and an evaporation chamber which is settled in an oven maintaining at 250°C . (Figure 4)

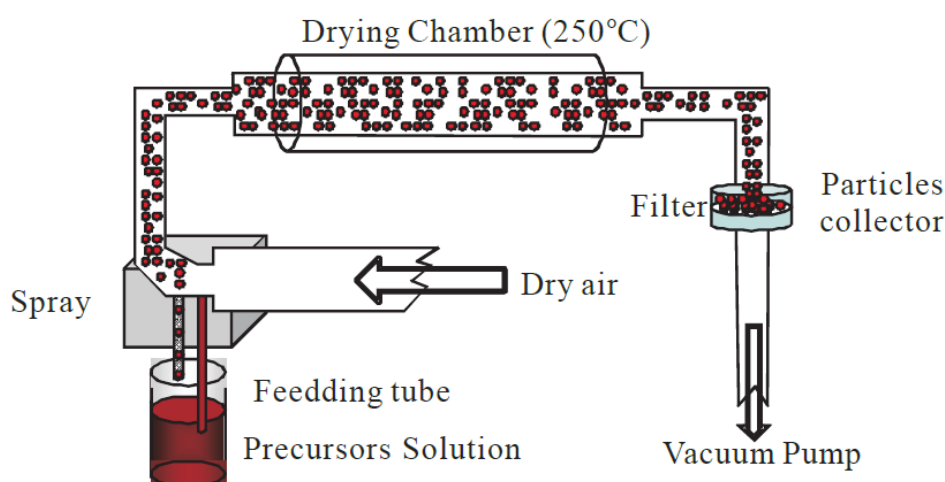


Figure 4. Schematic of the spray-drying method to preparation of organic-inorganic perovskite nanoparticles [25].

Droplets with initial mean diameter of $0.35\ \mu\text{m}$ are carried by dry air from the aerosol generator to the evaporation chamber. Dried particles are collected onto a $0.2\ \mu\text{m}$ cutoff Teflon filter and are stored at ambient temperature [25]. Transmission electron microscopy measurements show that these particles are spherical and their sizes are of the order of 50 to 500 nm.

2.1. Deposition techniques of inorganic–organic solar cells materials

The deposition technique is a quite important issue for perovskites studies, because many investigations and possible usages of organic-inorganic perovskite hybrids rely on the accessibility of simple and accurate thin film deposition method. But deposition of perovskite materials is often challenging because of the different chemical and physical property of the inorganic and organic portions [26]. For example, organic materials trend to be soluble in various solvents than inorganic section, this is causing chemical precursor solution preparation techniques (e.g., spin coating and dip coating) usually infeasible. For those reasons where the organic-inorganic hybrid is soluble, solution techniques are sometimes not suitable because of adverse wetting characteristics of some substrates, make deposition inhomogeneous. With respect to vacuum evaporation methods, the gradual heating of organic-inorganic compounds typically results in the decomposition or dissociation of the organic component at a lower

temperature or rapidly than that needed for evaporation of the metal halide component. Despite these evident difficulties, organic-inorganic perovskites represent a number of significant opportunities for thin film deposition or crystal growth of organic-inorganic hybrid perovskites, such as two-step dipping technique, spin coating, stamping, Langmuir-Blodgett (LB), two source thermal evaporation, solution evaporation and so on, which make possible the applications of perovskites as organic-inorganic electronic or photonic devices [27,28]. This section will offer a selected compilation of recent progress in this topic, demonstrating that a number of simple and effective methods can be utilized for the deposition of this considerable class of materials.

2.2. Spin-coating technique

Spin-coating is a very convenient technique widely applied to uniform thin film deposition. As it is shown in Figure 5, an amount of solution is dropped on the substrate which is fixed on the spin-coater, and then it is rotated at high speed in order to spread the fluid by centrifugal force. It can be considered as a special case of solution crystal growth, which allows the formation of highly oriented layered perovskites on a substrate, while the solvent is evaporating off. On the other hand, Spin-coating enables deposition of hybrid perovskites on various substrates, including glass, plastic, quartz, silicon and sapphire. Selection of the substrate, the solvent, the concentration of the hybrid in the solvent, the substrate temperature, and the spin speed are relevant parameters for this technique. In some cases, the wetting properties of the solution on the chosen substrate improved by pretreating the substrate surface with a suitable adhesion agent. In addition, post deposition low-temperature annealing ($T < 250^{\circ}\text{C}$) of the hybrid films is sometimes employed to improve crystallinity and phase purity. Mitzi et al. (2001b) comparing with the traditional deposition technique for inorganic semiconductors, spin-coating method doesn't require cumbersome equipment while it gives high-quality films in quite short time (several minutes) in room environment.

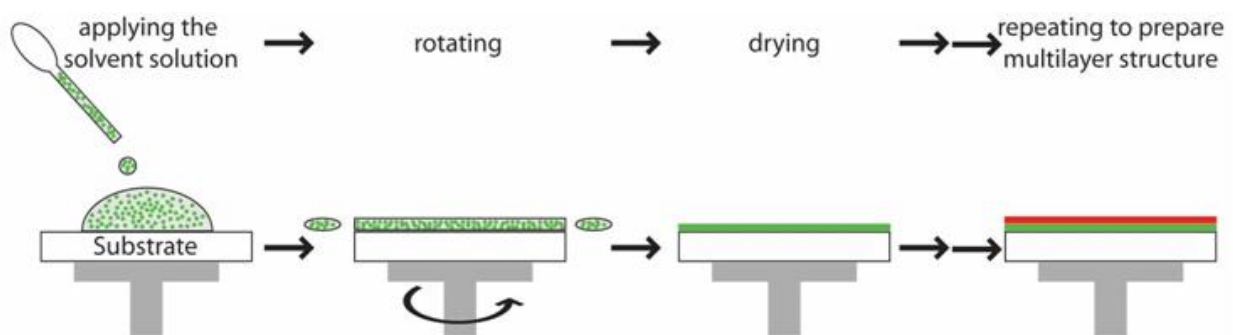


Figure 5. Schematic of the spin-coating process

Actually, in order to realize a layer with the desired thickness, can modify the concentration of perovskites solution and keep the other spin-coating parameters (spin speed, acceleration and spin duration) fixed. Generally, homogeneous 2D layered perovskites films with a thickness from 10 nm to 100 nm can be obtained by carefully selecting the parameters: less

concentrated solutions give thinner layers. The choice of the solvent is important because we need to consider the solubility for both the organic ammonium and the inorganic lead halide. Dimethylformamide (DMF) or Dimethyl sulfoxide (DMSO) are good solvents in which the perovskites usually have very high solubility. Some other solvents such as acetone, or acetonitrile can also be used. But solubility of perovskites in them is relatively poor (less than 5 wt%), and it takes too long to completely dissolve the solutes.

With the help of a profilometer or an Atomic force microscopy to measure the layer thickness, can draw a calibration curve (thickness as a function of concentration) and adjust the concentration of solution in order to produce the desired thickness. The spin-coated 2D layered perovskites films are very reproducible, and therefore they are appropriate to be deposited on devices.

2.3. Two-step dip-coating

In a sequential deposition procedure, a metal halide film is first deposited by vacuum evaporation or spin-coated from solution. Subsequently this film is transformed into the perovskite by dipping into a solution including the organic cation. Proper selection of solvent for the dipping solution is important. So that the organic salt is soluble in it, but the starting metal halide and the final organic-inorganic perovskite are not soluble.

In this case, the organic cations in solution intercalate into and rapidly react with the metal halide on the substrate and form a crystalline film of the desired hybrid, as it is described in Figure 6.

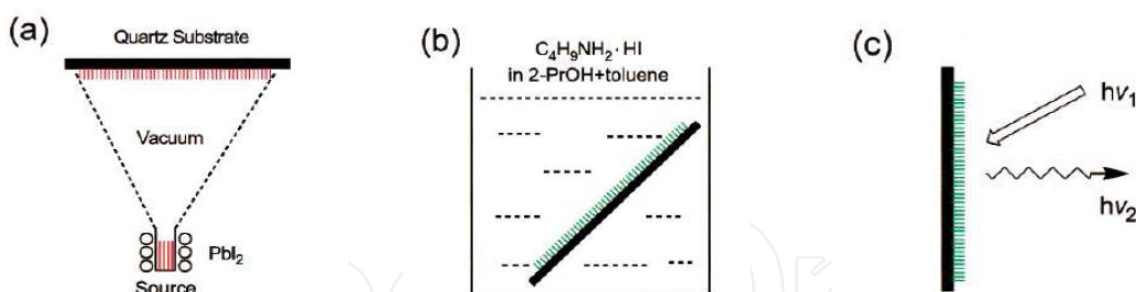


Figure 6. Schematic representation of the two-step dipping technique. In (a), a film of the metal halide is deposited onto a substrate using vacuum evaporation. The metal halide film is then (b) dipped into a solution containing the organic cation. The resulting film after dipping has the characteristic room temperature photoluminescence spectrum.

For the perovskite family, $(R-NH_3)_2 (CH_3NH_3)_{n-1} M_n I_{3n+1}$ ($R = \text{butyl or phenethyl}; M = \text{Pb or Sn}; n = 1 \text{ or } 2$), toluene/2-propanol mixture is a suitable solvent for the organic salt. The dipping times are relatively short: several seconds to several minutes, depending on the system. For example, a film of $(C_4H_9NH_3)_2 PbI_4$ was composed of a vacuum deposited film of PbI_2 (See figure 6 (a)) by dipping it into a butylammonium iodide solution, the reaction time was 1-3 min, which depends the PbI_2 film thickness (200-300 nm). After dip-coating, the films were instantly immersed in a rinse solution of the same solvent ratio as the initial dipping solution

without organic salt and dried in vacuum. Two-step dip-processing is a convenient method which can be used for a variety of organics and inorganics, even if they have incompatible solubility characteristics [26].

2.4. Thermal evaporation technique

The thermal evaporation method was firstly used by M. Era et al in 1997. They performed the dual-source vapor deposition by using lead iodide PbI_2 and organic ammonium iodide RNH_3I , in particular, the 2-phenylethylammonium iodide $\text{C}_6\text{H}_5\text{C}_2\text{H}_4\text{NH}_3\text{I}$.

As it is shown in Figure 7 organic and inorganic source were co-evaporated and deposited on fused quartz substrates. The pressure of evaporation chamber was about 10^{-6} Torr. In the preparation, the substrates were allowed to stand at room temperature. The spectrum of the vacuum deposited film corresponds well to those of single crystal and spin-coated films of the layered perovskite. Appearance of the strong exciton absorption and sharp exciton emission proves that the layered perovskite structure is organized in the vacuum deposited film [17].

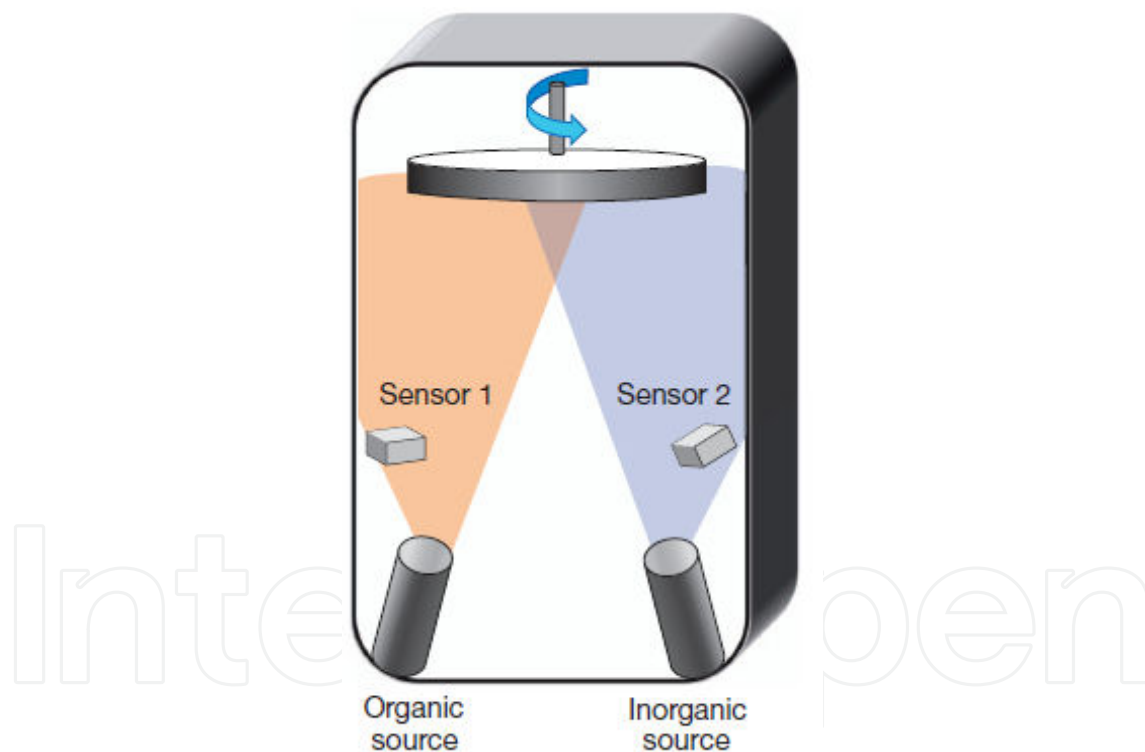


Figure 7. Schematic representation of the two-step dipping technique.

The benefits of this technique are that it is possible to precisely control the thickness and smoothness of the thin-film surfaces. However, this method has some disadvantage. It is often difficult to balance the organic and inorganic rates, an important criterion for achieving the correct compositions of the resulting perovskite films. Because each organic component easily contaminates the inside of the evaporation equipment is expected to limit the preparation of

various perovskites using different organic components. In addition, in some cases, the organic salt might not be thermally stable up to the temperatures required for evaporation, making this approach impracticable for a certain number of systems.

Furthermore, another method was developed to deposit perovskites thin films by using a single evaporation source. Mitzi et al. (1999). The apparatus for this single source thermal ablation (SSTA) technique consists of a vacuum chamber, with an electrical feed-through to a thin tantalum sheet heater, as shown in Figure 8.

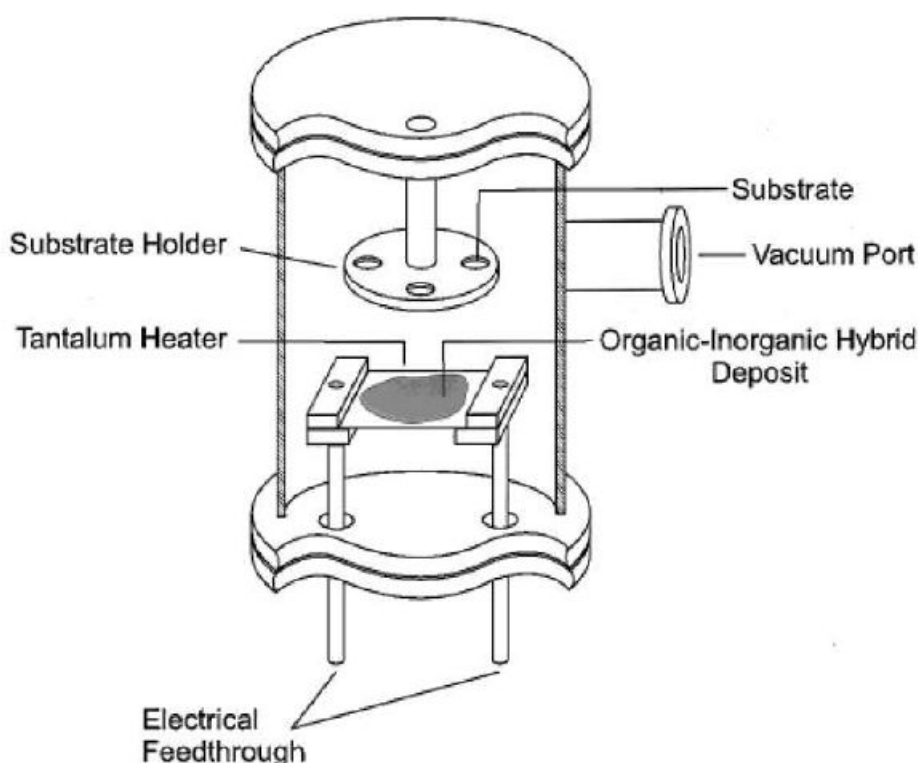


Figure 8. Schematic cross section of a single source thermal ablation chamber

Crystals, powder, or a concentrated solution of starting charge is placed on the heater. A suspension of insoluble powders in a quick-drying solvent are placed on the heater, because this enables the powder to be in better physical and thermal contact with, as well as more evenly dispersed across, the sheet. Under a suitable vacuum condition, the sheet temperature reaches approximately 1000 °C in 1-2 second, the entire starting charge ablates from the heater surface well before it incandesces. After ablation, the inorganic and organic parts reassemble on the substrates to produce optically clear films of the chosen product.

The key point to this procedure is that the ablation is quick enough for the inorganic and organic compounds to evaporate from the source at basically the same time and before the organic portion has had an opportunity to decompose. In many instances (particularly with

comparatively simple organic cations), the as-deposited films are crystalline and single phase at room temperature [26].

As show in Figure 9 Mingzhen Liu et al. compare the X-ray diffraction pattern of films of $\text{CH}_3\text{NH}_3\text{PbI}_{3-x}\text{Cl}_x$ both vapour-deposited and solution-cast onto compact TiO_2 -coated FTO-coated glass. The main diffraction peaks, assigned to the 110, 220 and 330 peaks at 14.12° , 28.44° and, respectively, 43.23° , are in same positions for both methods of films preparation, demonstrating that both techniques have produced the same organic-inorganic perovskite with an orthorhombic crystal structure [17]. Remarkably, focusing on the region of the (110) diffraction peak at 14.12° , there is only a small peak at 12.65° (the (001) diffraction peak for PbI_2) and no observable peak at 15.68° (the (110) diffraction peak for $\text{CH}_3\text{NH}_3\text{PbCl}_3$), indicating a high level of phase purity.

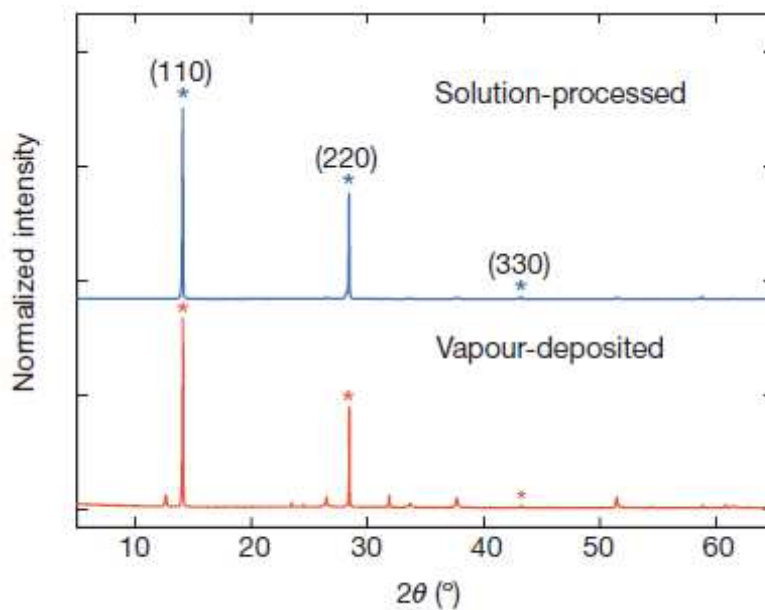


Figure 9. X-ray diffraction spectra of a solution-processed perovskite film (blue) and vapour deposited perovskite film (red) [17].

Figure 10 shows high-resolution scanning electron micrographs of $\text{CH}_3\text{NH}_3\text{PbI}_3$ perovskite film spin-cast on a glass/ITO/PEDOT:PSS substrate by Jun-Yuan Jeng et al. The crystal sizes in the cluster-domain regions of the perovskite are around 100–150 nm in $\text{CH}_3\text{NH}_3\text{PbI}_3$ perovskite film from butyrolactone solution and around 150–200nm in DMF solution [29].

Sanjun Zhang et al. performs atomic force microscopy (AFM) measurements for each spin-coated $(\text{R}-(\text{CH}_2)_n\text{NH}_3)_2\text{PbX}_4$ in order to examine the ability of the molecules to self-organize and define the surface roughness. Several examples of the obtained images are given in Figure 11. With the phenyl based semiconductor (2-phenylethanamine lead iodide), it was possible to cover the whole surface of the glass substrate; however, this was not the case for Cyclohexylmethanamine lead iodide, Myrtanylamine lead iodide and Cyclohexanamine lead bromide. It is clear that the surface roughness of the 2D phenyl-based is lower than that of the others [30].

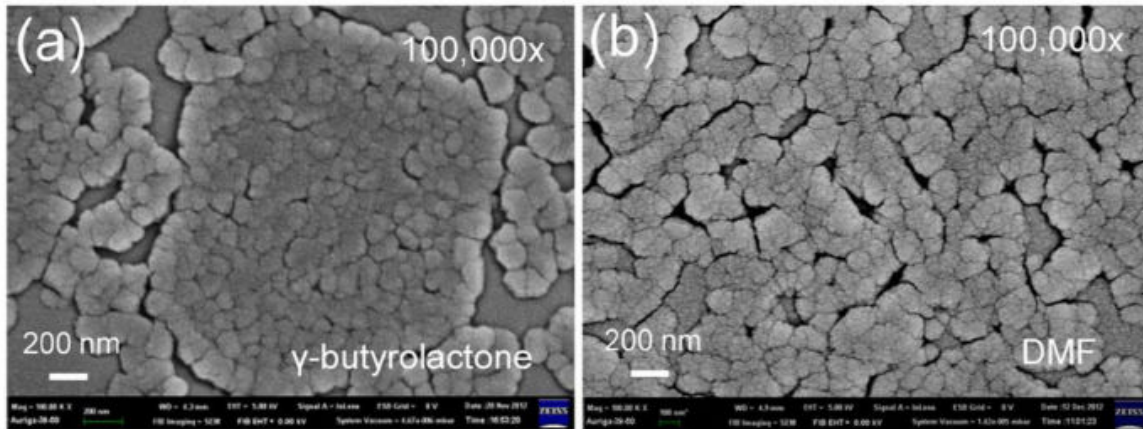


Figure 10. High-resolution scanning electron micrographs of $\text{CH}_3\text{NH}_3\text{PbI}_3$ perovskite film from (a) butyrolactone solution and (b) DMF solution [29].

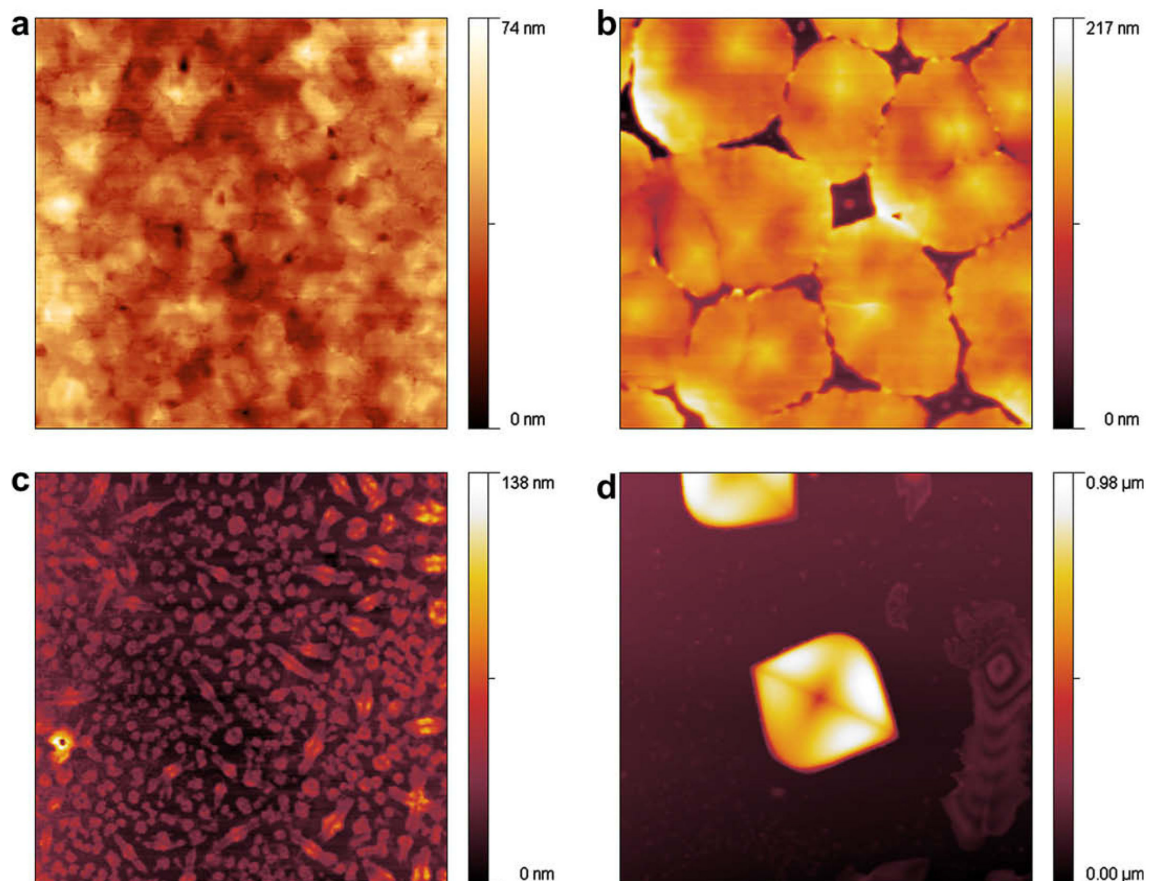


Figure 11. AFM images of 2D organic–inorganic semiconductor films: (a) 2-phenylethanamine lead iodide, (b) Cyclohexylmethanamine lead iodide, (c) Myrtanylamine lead iodide and (d) Cyclohexanamine lead bromide. The scales are $20 \mu\text{m} \times 20 \mu\text{m}$. Color coding of height is shown in the bar [30].

3. Electronic and optical properties of inorganic–organic solar cells materials

In the present decade organic-inorganic halide perovskite solar cells has been the most significant development in the field of photovoltaics for best bet at satisfying the need for high efficiencies while allowing for low cost manufacturing solutions. Since the first reports of stable solid state solar cells based on $\text{CH}_3\text{NH}_3\text{PbI}_3$ perovskite in middle of 2012, the power conversion efficiencies of the hybrid solar cells have already exceeded 17%, surpassing every other solar cells produced by solution-processing methods. The wide range of efficient perovskite solar cell device design indicated point towards a considerable semiconducting material with excellent electrical and optical properties. Early pioneering research [31] in organic-inorganic halides field has clearly shown that this hybrid materials are good candidates for low dimensional electronic systems with tunable properties, permitting for the development of newer perovskite materials for solar cells in addition to $\text{CH}_3\text{NH}_3\text{PbI}_3$. This section focuses on the recent progresses (*i.e.*, up to Feb 2014) in the area of perovskite solar cells as well as their electronic, optical properties and the dynamics of charge carriers [32]. We first review the electronic properties of this class of hybrid perovskites, followed by its progress as a solar cell material. Due to the rapid pace of research in this area, this section does not aim to be comprehensive but will highlight key work and findings.

Initial studies on the electronic band structures of organic-inorganic (3-D and low-dimensional) perovskites can be traced to the works as below, in 1996 koutselas and his team using band structure calculations by a semi-empirical method based on the extended Huckel theory and an *ab-initio* approach based on the Hartree-Fock theory [33]. Then T. Umebayashi *et. al.* using ultraviolet photoelectron spectroscopy and first principles density functional theory (DFT) band calculations for the room temperature cubic phase [34] and Chang team using first principles pseudopotential calculations in 2004 [35]. As shown in Figure 12 DFT calculations for the three dimensional $\text{CH}_3\text{NH}_3\text{PbI}_3$ crystal shown that the maxima of valence band consist of the Pb 6p - I 5p σ -anti-bonding orbital, while the minima of conduction band contains Pb 6p -I 5s σ anti-bonding and Pb 6p - I 5p π anti-bonding orbitals [34].

In line with respect to perovskite solar cells, interests in the DFT studies of 3D perovskites began renewed in earnest with the work of E. Mosconi together with F. De Angelis and their collaborators [37]. They calculated the band structure for $\text{CH}_3\text{NH}_3\text{PbX}_3$ (cubic phase) and the mixed halide $\text{CH}_3\text{NH}_3\text{PbI}_2\text{X}$ (tetragonal phase) ($\text{X} = \text{Cl}, \text{Br}$ and I) with the surrounding CH_3NH_3^+ , which were ignored in the earlier studies. Nevertheless, the organic component had little influence to the bandgap energy, of which is mainly determined by the $[\text{PbI}_4]^{6-}$ network. In addition, the authors highlight that their calculated bandgaps (by ignoring spin-orbit coupling (SOC)) are in good agreement with the experimental results. These findings are consistent with those in the later works by T. Baikie *et. al.*[37] and Y. Wang *et. al.* [38].

Figure 13 show the absorption spectra of the perovskite quantum well structures. Sharp resonance are due to the exciton state associated with the inorganic layers. So, by replacing different metal cations or halides in organic framework, the positions of the resonance can be manipulated[33, 39]. Room-temperature UV–vis absorption spectra for thin films of

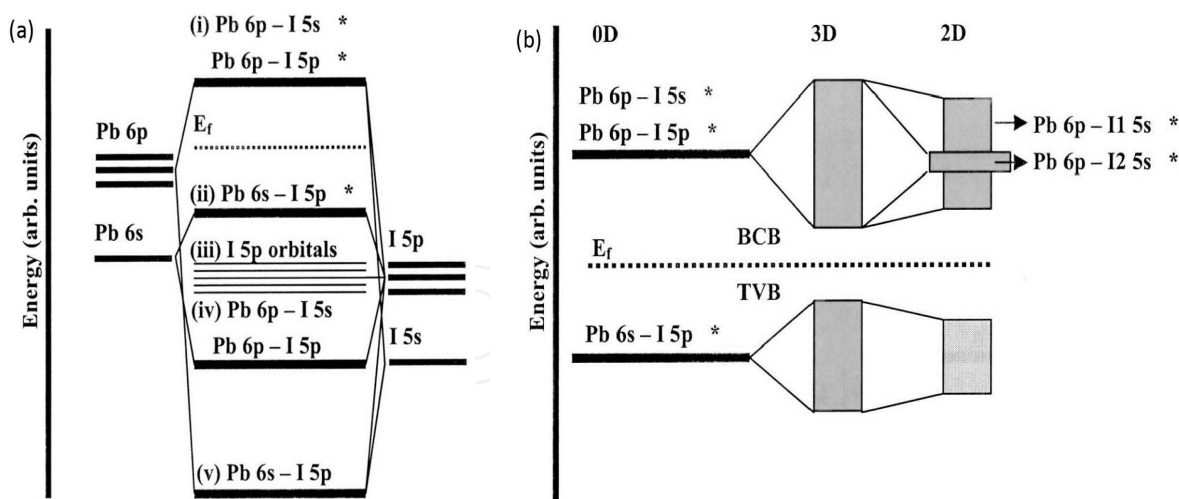


Figure 12. Bonding diagram of (a) $[\text{PbI}_6]^{4-}$ cluster (0-D), (b) $\text{CH}_3\text{NH}_3\text{PbI}_3$ (3-D) and (c) $(\text{C}_4\text{H}_9\text{NH}_3)_2\text{PbI}_4$ (2-D) at the top of the valence band and the bottom of the conduction band [34].

$(\text{C}_4\text{H}_9\text{NH}_3)_2\text{PbX}_4$ with (a) $\text{X} = \text{Cl}$, (b) $\text{X} = \text{Br}$, (c) $\text{X} = \text{I}$ are shown by Mitzi *et. al.* as shown in Figure 13. In each spectrum, the arrow demonstrates the position of the exciton absorption peak. The corresponding photoluminescence (PL) spectrum ($\lambda_{\text{ex}} = 370 \text{ nm}$) is shown by the dashed curve in figure 13-c. A Stokes shift of about 15nm between peaks of the absorption and emission peaks for the excitonic transition is notable.

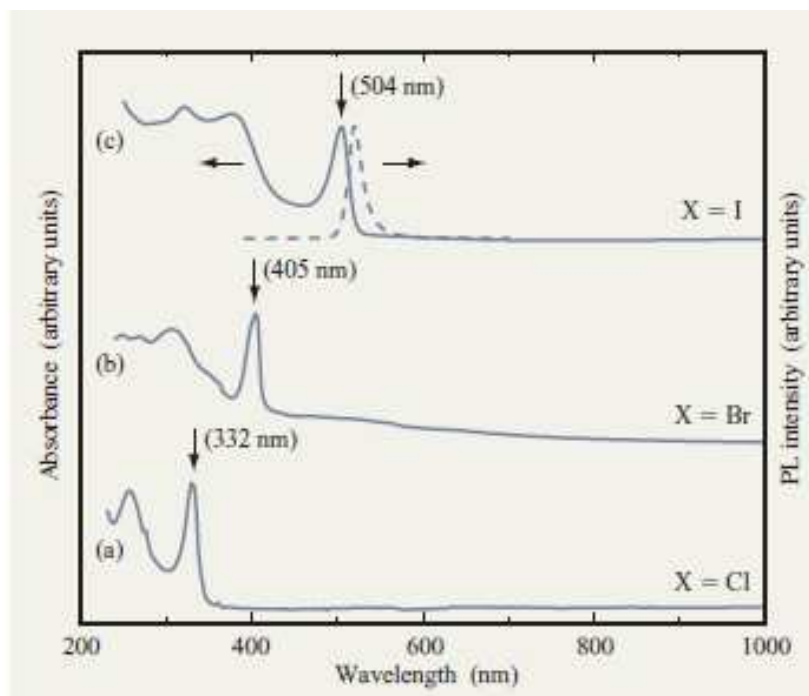


Figure 13. Room-temperature UV–vis absorption spectra for thin films of $(\text{C}_4\text{H}_9\text{NH}_3)_2\text{PbX}_4$ with (a) $\text{X} = \text{Cl}$, (b) $\text{X} = \text{Br}$, (c) $\text{X} = \text{I}$ [39].

Because of the two-dimensionality of the inorganic structure, coupled with the dielectric modulation between the organic and inorganic layers, the strong binding energy of the excitons arise, which enables the optical features to be observed at room temperature. Also strong photoluminescence, nonlinear optical effects and tunable polariton absorption arise from the large exciton binding energy and oscillator strength [39].

The excitonic absorption and light emission closely relate to the different metal halide in 2D perovskite. For instance, the absorption and photoluminescence of $(C_5H_4CH_2NH_3)_2PbX_4$ varied with substitution of different halogens. As show in Figure 14, the light emissions change by green to blue and blue to ultraviolet when $X=I \rightarrow Br \rightarrow Cl$ [40]. The small FWHM of the peaks and very small Stokes shift between the UV-vis absorption and PL emission spectra are the signature of exciton.

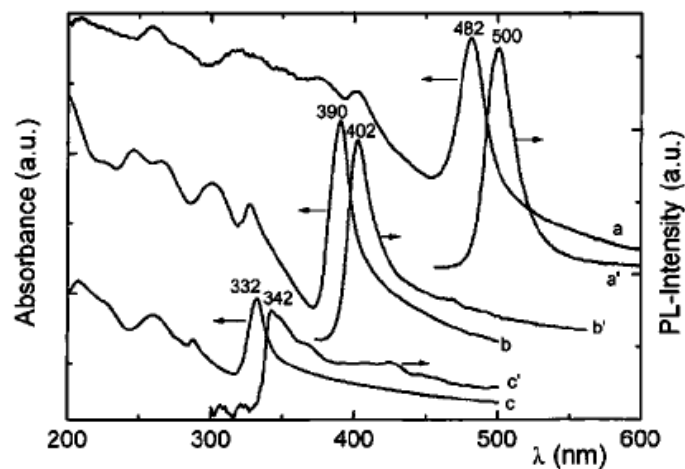


Figure 14. Optical absorption of (a, b, c) and photoluminescence (a', b', c') spectra for $(C_5H_4CH_2NH_3)_2PbI_4$ (a, a'), $(C_5H_4CH_2NH_3)_2PbBr_4$ (b, b') and $(C_5H_4CH_2NH_3)_2PbCl_4$ (c, c')

The noticeable feature of the exciton state in this system is the extremely large binding energy. For example, the binding energy in $(C_6H_5-C_2H_4NH_3)_2PbI_4$ are 220 meV. For comparison, the exciton state in bulk PbI_2 has a binding energy of only 30 meV. According to the other studies the larger binding energy is due to the unusual alternating organic–inorganic layered structure and the effect of dielectric confinement. The screening of carriers in organic layer is small due to lower dielectric constant of the inert organic molecules. Also lower dielectric constant of organic layer lead to enhancement of the coulomb interaction between electron and hole (higher exciton binding energy) [40].

As already pointed out in a lot of published works it is interesting to compare the luminescence and absorption properties of the organic–inorganic compounds. As revealed, extensive studies of the excitonic properties of lead halide based organic–inorganic materials $(R-NH_3)_2PbX_4$ have been performed. The measured absorption and photoluminescence wavelengths of $(R-NH_3)_2PbI_4$ and $(R-NH_3)_2PbBr_4$ reported in the literature are summarized in Table 1. Using different organic chains (e.g. simple saturated organic chains and unsaturated chains

including aromatic rings and delocalized p electrons) demonstrate enhancement of the photoluminescence and the binding energy of excitons. For the saturated alkylammonium chains organic layers, the length of organic chain and the width of the PbI_4 wells does not affect the excitonic properties. This is due to the small difference between the dielectric constants of the inorganic and organic layers which leads to a rather weak impact of the dielectric confinement (see, for instance, the work of Ishihara et al. on $(\text{C}_n\text{H}_{2n+1}\text{NH}_3)\text{PbI}_4$ with $n = 4, 6, 8, \dots, 12$). In contrast, when the organic chains consist of aromatic rings and delocalized p electrons, the binding energy of exciton is low because of the difference between the organic and inorganic dielectric constants (dielectric confinement effect) and the luminescence peak shows red shift [41-44]. This dependence of the saturated/unsaturated nature of the organic chains is summarized in Table 1.

Comparison of the absorption and photoluminescence peak wavelengths and the exciton binding energy of $(\text{NH}_3(\text{CH}_2)_6\text{NH}_3)\text{PbBr}_4$ with those of the homologous bromide and iodide compounds as shown in Table 1. It is clear that the exciton binding energy of compounds (I) and (II) containing saturated organic chains are almost the same (about 180 meV). On the other hand, compounds (III) and (IV) containing unsaturated organic chains, exhibit much lower exciton binding energy. The homologous iodide compound (V) with the same (saturated) organic chain as $(\text{NH}_3(\text{CH}_2)_6\text{NH}_3)\text{PbBr}_4$ shows strong photoluminescence at room temperature. The efficient emitted photoluminescence is observable by naked eyes

References	Stokes shift (exciton binding energy)	PL (nm)	Absorption (nm)	Compound
[41]	nm (181 meV) 22	402	380	$(\text{NH}_3(\text{CH}_2)_6\text{NH}_3)\text{PbBr}_4$ (saturated chain)
[42]	nm (177 meV) 25	430	405	$(\text{C}_4\text{H}_9\text{NH}_3)_2\text{PbBr}_4$ (saturated chain)
[41]	nm (107 meV) 17	436	419	$(\text{C}_5\text{H}_7\text{NH}_3)\text{PbBr}_4$ (unsaturated chain)
[43]	nm (127 meV) 15	417	399	$(\text{R-PhNH}_3)\text{PbBr}_4$ (unsaturated chain)
[44]	nm (330 meV) 56	555	–	$(\text{NH}_3(\text{CH}_2)_6\text{NH}_3)\text{PbI}_4$ (saturated chain)

Table 1. Absorption, photoluminescence wavelengths and Stokes shifts of some reported compounds.

4. Photovoltaic effect in inorganic–organic perovskite solar cells

Solar power is the one of the world's most abundant energy resource and daily input of this energy to the earth's surface is enough to cover our energy needs, but efficient and cost-effective ways of converting it to electricity, have remained as one of the scientist's challenges.

Photovoltaic cells are the most promising device for directly converting the photons to electricity and it has been extensively studied in the past 50 years using various combinations of inorganic semiconductors or organic sensitizers. For photovoltaic energy to become competitive with fossil fuels and to capture a worthy place at energy markets, it is necessary to reduce the total cost of solar energy conversion by increasing their power conversion efficiencies or by reducing the cost of photovoltaic cells.

Today there is a lot of material used in photovoltaic structure and installed around the world. The photovoltaic market is currently dominated by crystalline Si solar cells with efficiencies close to 20% that known as First Generation of Solar Cells. This generation that have more than 150 micrometer thick, have the highest efficiency in all type of Solar cells that manufactured, but take a lot of energy to produce and therefore the cost of manufacturing is too high.

As cost-effective devices, thin film solar cell those containing a few micrometers of inorganic materials that known as second generation can be introduced. With a thin photovoltaic film, optical management is an important key for harvesting light while ensuring high efficiency. Thin film solar cell often limit light-harvesting ability because of their materials low absorption coefficients and narrow absorption bands. At least, these flexible cells have lower material costs, but they are also less efficient.

Alternative “third generation” technologies such as dye sensitized solar cells, organic photovoltaics and quantum dot solar cells in both electrochemical and solid-state structures, assure low cost solar power because of low cost fabrication methods based on solution-processing techniques such as blade coating, screen printing and spraying, but high bandgap light absorption by these types has not allowed high performance in quantum conversion and photovoltaic generation.

The first observation of photocurrents in oxide perovskite material can date back to 1956 [1] that have been widely studied. David B. Mitzi in 1990 used organometal halide perovskites in LED [2] and thin-film field-effect transistors [3] and demonstrated its high efficiency as light emitters. Given that we know the good light emitter is a good light absorber, perovskites materials because of their light absorption efficiently over a broad spectrum is convenient option as photovoltaic materials.

Also, because perovskite can directly deposited from solution, manufacturing costs is lower than another type of solar cells. But it should be noted that manufacturing cost could rise due to encapsulation process. Therefore, perovskites could resolve the solar cell industry by matching the output of silicon cells at a lower price than that of thin film, because of their low-cost materials and manufacturing process.

For first time in 2009, perovskites were used as solar cell [4]. As show in Figure 15 this device are built upon the architectural basis for DSSCs and achieved 3.8% efficiencies in a liquid electrolyte configuration where the absorber was regarded as a QDs deposited on TiO_2 . The efficiency was further improved to 6.5% but the enormous drawback to this types, regardless of their low efficiency, were had dissolution of liquid electrolyte away the perovskite that cause short stability for device.

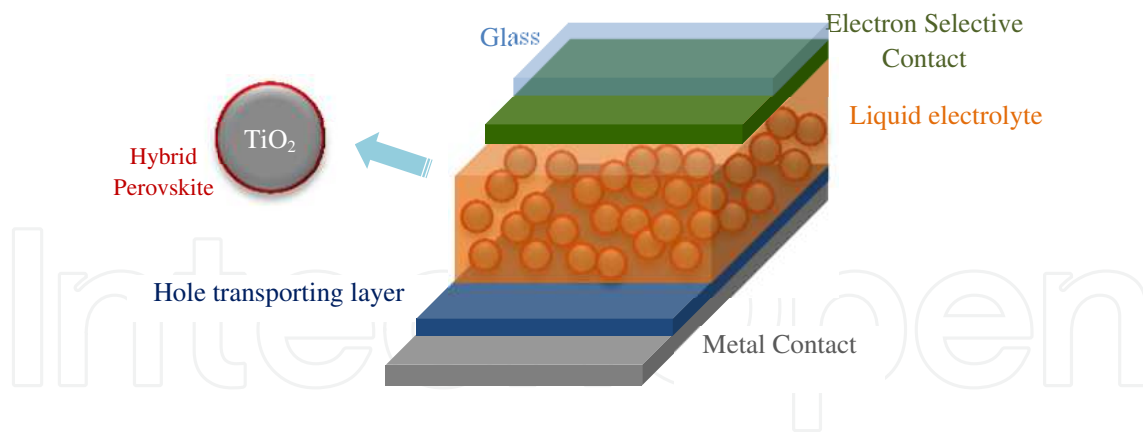


Figure 15. Schematic of first perovskites solar cell

Introducing of Solid Hole Transporting Layer (HTL) by Nam-Gyu Park and Gratzel [5], and replace liquid electrolyte by it, solve this problem in 2012 and rose the efficiency to 9%. (Figure 16)

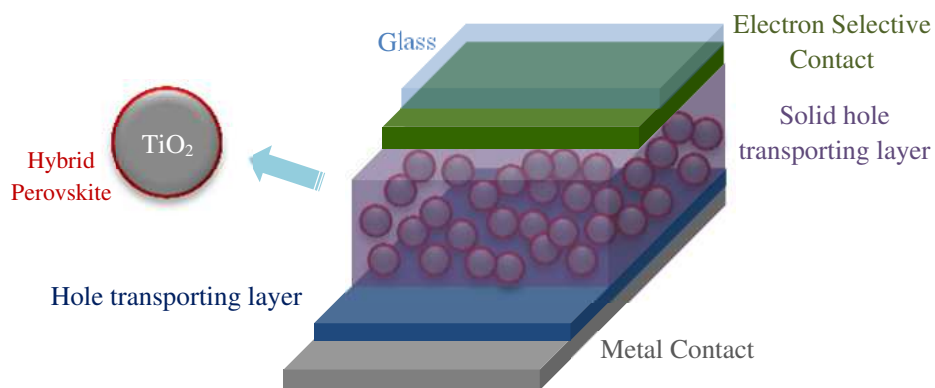


Figure 16. Nam-Gyu Park and Gratzel perovskites solar cell

In the late 2012s, research topics towards to materials engineering and switch structure by manufacturing methods to increase the Efficiency of these type of solar cells. Henry Snaith [6] in Oxford University Switched TiO₂ to an insulating Aluminum oxide scaffold in Gratzel perovskites solar cell that show in Figure 17. This switch, surprisingly increase efficiency to 10.9%.



Figure 17. Switching TiO₂ to an Al₂O₃ in Gratzel perovskites solar cell

On the other hand, Snaith and coworkers [17] demonstrated efficient planar solar cells of $\text{CH}_3\text{NH}_3\text{PbI}_{3-x}\text{Cl}_x$ formed by dual source evaporation of PbCl_2 and $\text{CH}_3\text{NH}_3\text{I}$. The film was evaporated on a compact TiO_2 layer (as an electron transport layer) and then a Spiro-OMeTAD layer (as a hole transport layer) was spin coated over it (Figure 18). The evaporated films containing crystalline structures on the length scale of hundreds of nanometers are enormously uniform [32].

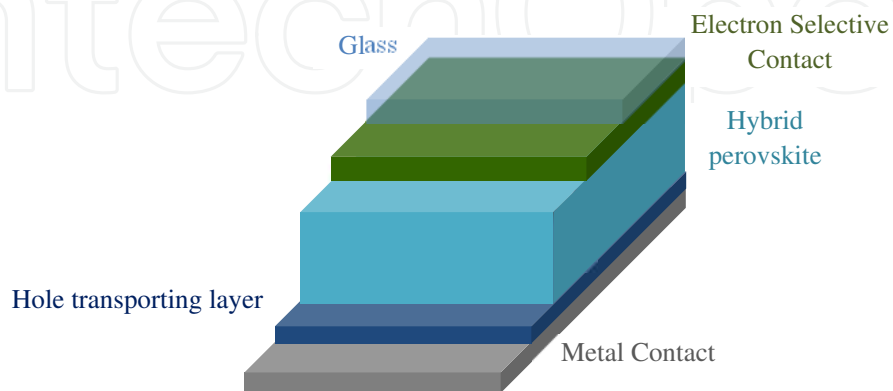


Figure 18. Schematic of Snaith hybrid perovskite solar cell

Finally they reported 15.4% efficiency for their device and another research in this area, reported the difference efficiency by using different material for example PbI_2 that Graetzel and Bolink [7] used (device efficiency was 12.04 %) or difference evaporation method for example as show in Figure 19 employs both solution based deposition and vapor phase transformation by Graetzel [21] and coworkers, that report 12.1 % efficiency for their device.

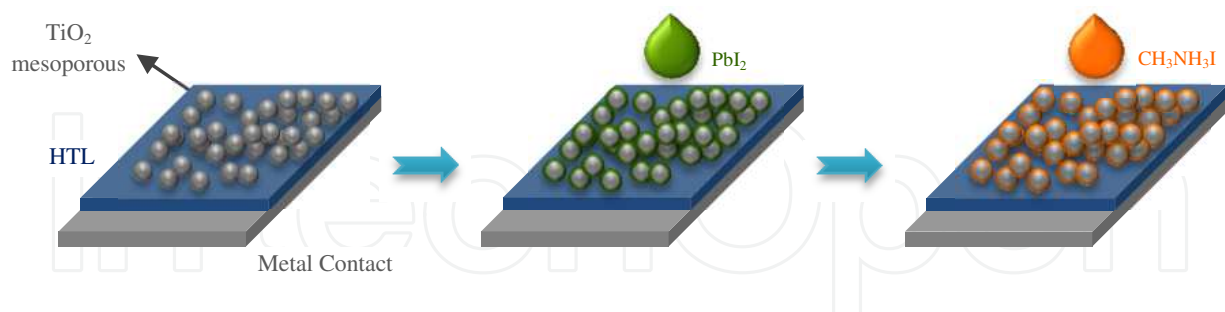


Figure 19. Graetzel sticks with the TiO_2 structure and tinkered with the deposition step.

These deposition techniques had two important drawbacks: first challenging for large-scale industrial production and second is that the all-solution process results in decreased film quality, and the vacuum process requires expensive equipment and uses a great deal of energy. Yang Yang [16] from UCLA university present new method named "Vapor-assisted solution process" that organic material infiltrates the inorganic matter and forms a compact perovskite film. These films is significantly more uniform than the films produced by the wet technique (Figure 20).

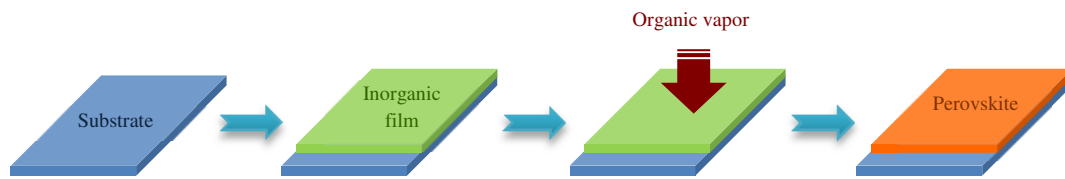


Figure 20. Vapor-assisted solution process

In conjunction with these exciting device-centric advancements, fundamental studies into the photoexcited species and their photogeneration and recombination dynamics in perovskites also began in earnest.

At least one of the remaining question is “Is the Solar Cell Excitonic?” Perovskite solar cell had similar diffusion lengths for electron and hole that average is about 100 to 300 nm [8] that put these cells in conventional solar cell class. On other hand either indicate similar mobilities for both holes and electrons [9] and this classify these cells in excitonic solar cell group (Figure 21).

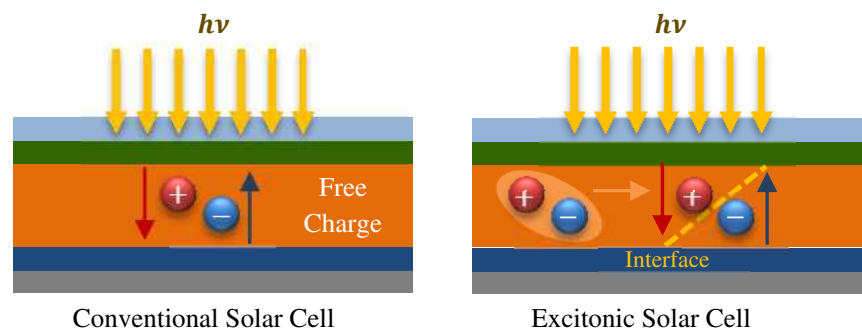


Figure 21. Schematic of conventional and excitonic solar cell

Accordingly, due to the common properties of these types of solar cells, between Conventional and excitonic solar cell, researchers cannot exactly determine whether the photoexcited species are excitons or free charges.

5. Conclusion

In this section we have presented the synthesis and characterization of organic-inorganic hybrid perovskite. Hybrid organic-inorganic materials represent an alternative to present materials as they guarantee improved optical and electronic properties by combining organic and inorganic components together. The unusual features and versatile characteristics of hybrid organic-inorganic perovskites open up promising applications in many fields such as electronics, optics, optoelectronics, mechanics, environment, medicine and biology. The application of these materials in the solar cells as a novel class of low-cost materials for high efficiency hybrid semiconductor photovoltaic cells has been explained in more detail.

Author details

Sohrab Ahmadi Kandjani*, Soghra Mirershadi and Arash Nikniaz

*Address all correspondence to: s_ahmadi@tabrizu.ac.ir

Research Institute of Applied Physics and Astronomy (RIAPA), University of Tabriz, Iran

References

- [1] Agranovich V, Gartstein Y N, Litinskaya M. Hybrid Resonant Organic-Inorganic Nanostructures for Optoelectronic Applications. *Chemical Reviews* 2011; 111 5179–5214.
- [2] Pope M, Kalmann H, Magnante P. Electroluminescence in Organic Crystals *The Journal of Chemical Physics* 1963; 38 2042–2043.
- [3] Agranovich V, Atanasov R, Bassani F. Hybrid interface excitons in organic-inorganic quantum wells. *Solid State Communications* 1994; 92 295–301.
- [4] Agranovich V, La Rocca G C, Bassani F. Efficient electronic energy transfer from a semiconductor quantum well to an organic material. *JETP Letters* 1997; 66 748–751.
- [5] Agranovich V, Benisty H, Weisbuch C. Organic and inorganic quantum wells in a microcavity: Frenkel-Wannier-Mott excitons hybridization and energy transformation. *Solid State Communications* 1997; 102 631–636.
- [6] Dammak T, Elleuch S, Bougzhala H, Mlayah A, Chtourou R, Abid Y. Synthesis, vibrational and optical properties of a new three-layered organic inorganic perovskite ($C_4H_9NH_3$)₄Pb₃I₄Br₆. *Journal of Luminescence* 2009; 129 893–897.
- [7] Mitzi D, Field C, Harrlson W, Guloy A. Conducting tin halides with a layered organic-based perovskite structure. *Nature* 1994; 369 467–469.
- [8] Hong X, Ishihara T, Nurmikko A V. Photoconductivity and electroluminescence in lead iodide based natural quantum well structures. *Solid State Communications* 1992; 84 657–661.
- [9] Cheng Z Y, Wang Z, Xing R B, Han Y C, Lin J. Patterning and photoluminescent properties of perovskite-type organic/inorganic hybrid luminescent films by soft lithography. *Chemical Physics Letters* 2003; 376 481–486.
- [10] Tabuchi Y, Asai K, Rikukawab M, Sanuib K, Ishigure K. Preparation and characterization of natural lower dimensional layered perovskite-type compounds. *Journal of Physics and Chemistry of Solids* 2000; 61 837–845.

- [11] Kitazawa N, Watanabe Y. Optical properties of natural quantum-well compounds $(\text{C}_6\text{H}_5\text{-C}_n\text{H}_{2n}\text{-NH}_3)_2\text{PbBr}_4$ ($n=1\text{--}4$). *Journal of Physics and Chemistry of Solids* 2010; 71 797–802.
- [12] Kitazawa N, Yaemponga D, Aono M, Watanabe Y. Optical properties of organic–inorganic hybrid films prepared by the two-step growth process. *Journal of Luminescence* 2009; 129 1036–1041.
- [13] Ema K, Ishi J, Kunugita H, Ban T, Kondo T. All-optical serial-to-parallel conversion of Tbits/s signals using a four-wave-mixing process. *Optical and Quantum Electronics* 2001; 33 1077–1087.
- [14] Brehier A, Parashkov R, Lauret J S, Deleporte E. Strong exciton–photon coupling in a microcavity containing layered perovskites semiconductors. *Applied Physics Letters* 2006; 89 171110-1.
- [15] Era M, Morimoto S, Tsutsui T, Saito S. Organic–inorganic heterostructure electroluminescent device using a layered perovskite semiconductor $(\text{C}_6\text{H}_5\text{C}_2\text{H}_4\text{NH}_3)_2\text{PbI}_4$. *Applied Physics Letters* 1994; 65 676–678.
- [16] Shibuya K, Koshimizu M, Takeoka Y, Asai, K. Scintillation properties of $(\text{C}_6\text{H}_{13}\text{NH}_3)_2\text{PbI}_4$: exciton luminescence of an organic/inorganic multiple quantum well structure compound induced by 2.0 MeV protons. *Nuclear Instruments and Methods B* 2002; 194 207–212.
- [17] Liu M, Johnston M B, Snaith H J. Efficient planar heterojunction perovskite solar cells by vapour deposition. *Nature* 2013; 501 395–398.
- [18] Snaith H J. Perovskites: The Emergence of a New Era for Low-Cost, High-Efficiency Solar Cells. *The Journal of Physical Chemistry Letters* 2013; 4 3623–3630.
- [19] Edri E, Kirmayer S, Cahen D Hodes G. High Open-Circuit Voltage Solar Cells Based on Organic–Inorganic Lead Bromide Perovskite *The Journal of Physical Chemistry Letters* 2013; 4 897–902.
- [20] Heo J H, Im S H, Noh J H, Mandal T N, Lim C S, Chang J A, Lee Y H, Kim H J, Sarkar A, Nazeeruddin M K, Gratzel M, Seok S. Efficient inorganic–organic hybrid heterojunction solar cells containing perovskite compound and polymeric hole conductors. *Nature photonics* 2013; 7 486–491.
- [21] Burschka J, Pellet N, Moon S J, Humphry-Baker R, Gao P, Nazeeruddin M K, Gratzel M. Sequential deposition as a route to high-performance perovskite-sensitized solar cells; *Nature* 2013. 499, 316– 319.
- [22] Kitazawa N, Aono M Watanabe Y. Excitons in organic–inorganic hybrid compounds $(\text{C}_n\text{H}_{2n+1}\text{NH}_3)_2\text{PbBr}_4$ ($n=4, 5, 7$ and 12); *Thin Solid Films* 2010. 518 3199–3203.

- [23] Liang L, Zhang J, Zhou Y, Xie J, Zhang X, Guan M, Pan B and Xie Y 2013 High-performance flexible electrochromic device based on facile semiconductor-to-metal transition realized by $\text{WO}_3 \cdot 2\text{H}_2\text{O}$ ultrathin nanosheets; *Scientific reports* 2013. 1936 1-8.
- [24] Tabuchi Y, Asai K, Rikukawa M, Sanui K, Ishigure K. Preparation and characterization of natural lower dimensional layered perovskite-type compounds; *Journal of Physics and Chemistry of Solids* 2000. 61 837–845.
- [25] Wei Y. Synthesis and optical properties of self-assembled 2D layered organic-inorganic perovskites for optoelectronics. PhD thesis. The Quantum and Molecular Photonics Laboratory, France 2012.
- [26] Mitzi D B. Thin-Film Deposition of Organic-Inorganic Hybrid Materials; *Chemistry of Materials* 2001. 13 3283-3298.
- [27] [27].Kitazawa N, Enomoto K, Aono M, Watanabe Y. Optical Properties of $(\text{C}_6\text{H}_5\text{C}_2\text{H}_4\text{NH}_3)_2\text{PbI}_{4-x}\text{Br}_x$ ($x=0-4$) mixed-crystal doped PMMA films; *Journal of Materials Science* 2004. 39 749–751.
- [28] Dwivedi V K, Baumberg J, Vijaya Prakash G. Direct deposition of inorganic organic hybrid semiconductors and their template-assisted microstructures; *Materials Chemistry and Physics* 2013. 137 941–946.
- [29] Jeng J Y, Chiang Y F, Lee M H, Peng S R, Guo T F, Chen F, Wen T C. Methylammonium lead iodide perovskite/fullerene-based hybrid solar cells; *SPIE Newsroom* 2014. 10.1117/2.1201307.005033.
- [30] Zhang S, Lanty G, Lauret J S, Deleporte E, Audebert P, Galmiche L. Synthesis and optical properties of novel organic-inorganic hybrid nanolayer structure semiconductors; *Acta Materialia* 2009. 57 3301–3309.
- [31] Mitzi D B. *Progress in Inorganic Chemistry*, John Wiley & Sons, Inc., 2007, DOI: 10.1002/9780470166499.ch1, pp. 1-121.
- [32] Sum T C, Mathews N. Advancements in Perovskite Solar Cells: Photophysics behind the Photovoltaics; *Energy & Environmental Science* 2014. 7 2518-2534
- [33] Koutselas I B, Ducasse L, Papavassiliou G C. Electronic properties of three- and low-dimensional semiconducting materials with Pb halide and Sn halide units ; *Journal of Physics: Condensed Matter* 1996. 8 1217-1227.
- [34] Umebayashi T, Asai K, Kondo T, Nakao A. Electronic structures of lead iodide based low-dimensional crystals; *Physical Review B* 2003 67.....
- [35] Chang Y H, Park C H, Matsuishi K. First-Principles Study of the Structural and the Electronic Properties of the Lead-Halide-Based Inorganic-Organic Perovskites $(\text{CH}_3\text{NH}_3)\text{PbX}_3$ and CsPbX_3 ($X = \text{Cl}, \text{Br}, \text{I}$) ; *Journal of the Korean Physical Society* 2004. 44 889-893.

- [36] Mosconi E, Amat A, Nazeeruddin M K, Gratzel M, De Angelis F. First-Principles Modeling of Mixed Halide Organometal Perovskites for Photovoltaic Applications; *The Journal of Physical Chemistry C* 2013. 117 13902-13913.
- [37] Baikie T, Fang Y N, Kadro J M, Schreyer M, Wei F X, Mhaisalkar S J, Graetzel M, White M T. Synthesis and crystal chemistry of the hybrid perovskite $(\text{CH}_3\text{NH}_3)\text{PbI}_3$ for solid-state sensitised solar cell applications; *Journal of Materials Chemistry A* 2013. 1 5628-5641.
- [38] Wang Y, Gould T, Dobson J F, Zhang H, Yang H, Yao X, Zhao H. Density functional theory analysis of structural and electronic properties of orthorhombic perovskite $\text{CH}_3\text{NH}_3\text{PbI}_3$; *Physical Chemistry Chemical Physics* 2014. 16 1424-1429.
- [39] Mitzi D B, Chondroudis K, Kagan C R. Organic–inorganic electronics; *IBM Journal of Research and Development* 2001. 45 29-45.
- [40] Cheng Z, Lin J. Layered organic–inorganic hybrid perovskites: structure, optical properties, film preparation, patterning and templating engineering *Crystal Engineer Community* 2010. 12, 2646–2662.
- [41] Dammak T, Fourati N, Boughzala H, Mlayah A, Abid Y. X-ray diffraction, vibrational and photoluminescence studies of the self-organized quantum well crystal $\text{H}_3\text{N}(\text{CH}_2)_6\text{NH}_3\text{PbBr}_4$; *Journal of Luminescence* 2007. 127 404- 408.
- [42] Yamamoto Y, Oohata G, Mizoguchi K, Ichida H, Kanematsu Y. Photoluminescence of excitons and biexcitons in $(\text{C}_4\text{H}_9\text{NH}_3)_2\text{PbBr}_4$ crystals under high excitation density; *physica status solidi (c)* 2012. 9 2501-2504.
- [43] Cheng Z Y, Wang H F, Quan Z W, Lin C K, Lin J, Han Y C, Layered organic–inorganic perovskite-type hybrid materials fabricated by spray pyrolysis route; *Journal of Crystal Growth* 2005. 285 352-357.
- [44] Goto T, Ohshima N, Mousdis G A, Papavassiliou G C. Excitons in a single two-dimensional semiconductor crystal of $\text{H}_3\text{N}(\text{CH}_2)_6\text{NH}_3\text{PbI}_4$; *Solid State Communications* 2001. 117, 13-16.
- [45] Chen F S, Optically induced changes in refractive index in LiNbO_3 . *Journal of Applied Physics* 1969; 40 3389–3396.
- [46] Mitzi D B, Chondroudis K. Electroluminescence from an Organic–Inorganic Perovskite incorporating a quaterthiophene dye within lead halide perovskite layers. *Chemical Material* 1999; 11 (11), pp 3028–3030.
- [47] Kagan C R, Mitzi D B, Dimitrakopoulos C D. Organic-inorganic hybrid materials as semiconducting channels in thin-film field-effect transistors, *Science* 1999; 286 (5441), 945-947.
- [48] Bulkin B. Perovskites: the future of solar power?, *The Guardian* 2014; <http://www.theguardian.com/sustainable-business/perovskites-future-solar-power>

- [49] Gratzel M, Park NG. Lead iodide perovskite sensitized all-solid-state submicron thin film mesoscopic solar cell with efficiency exceeding 9%, *Science Rep.* 2012;2591.
- [50] SnaithHJ, LeeMM. Efficient hybrid solar cells based on meso-superstructuredorgano-metal halide perovskites, *Science* 2012; 338(6107)643-7.
- [51] MalinkiewiczO, YellaA, LeeY H, EspallargasG M, GraetzelM, NazeeruddinM K,Bo-linkH. Perovskite solar cells employing organic charge-transport layers, *J. Nat Photonics*2014; 8, 128-132.
- [52] Stranks S, Eperon G, Grancini G, Menelaou C, Alcocer M, Leijtens T, Herz L, Petroz-zaA, Snaith H. Electron-hole diffusion lengths exceeding 1 micrometer in an organo-metaltrihalideperovskite absorber, *Science* 2013; 342(6156)341-4.
- [53] Gregg B A. Excitonic solar cells, *J. Phys. Chem. B* 2003; 107(20) 4688–4698.